Failure Mechanisms in PMMA/ATH Acrylic Casting Dispersion

Shihua Nie[1], Cemal Basaran[2], Clyde S. Hutchins[3], and Hale Ergun[4]

[1,2]Department of Civil, Structural and Environmental Engineering
State University of New York at Buffalo, Buffalo, NY 14260
Email: cjb@eng.buffalo.edu
[3]Dupont Surfaces, Yerkes R&D Lab
4 Dept. of Civil Eng., Istanbul Technical University, Turkey

Abstract: Acrylic casting dispersion is used to fabricate particulate composites such as poly-methyl methacrylate (PMMA) filled with a fine dispersion alumina trihydrate (ATH). This composite is subjected to severe temperature variations during in-service conditions, giving rise to high thermal stresses which lead to failure by cracking. The influence of the interfacial bond strength between a particle and the matrix on the failure mechanism of acrylic casting dispersion has been investigated using *in situ* observations during tensile and compressive loadings. Experiments show that the failure in pure tension occurs differently than in flexure loading where the failure process is believed to be more complex. During tensile loading, it is observed that macroscopic fracture is initiated in the clusters of the reinforcing particles because of the strong interfacial bonding strength between the filler particles and matrix. For weak interfacial bond strength, the macroscopic fracture is initiated by separation of filler agglomerates from the matrix.

Keywords: Particulate composites, failure mechanism, damage mechanics, particle filled composites, Nano indentation

1. INTRODUCTION

The rapid growth of activity in the composites industry continues to create a need for materials that meet the difficult demands for high performance at an economical cost. Particulate composites have been popular in many other engineering applications because of their low production cost and significantly improved material properties compared with the matrix material. Particle composites have properties such as increased stiffness, a reduction in thermal expansion and an improvement in creep resistance and fracture toughness. A particulate composite consists of a physical mixture of particles and a binder material, and has various choices as its particles and matrix material (Chawla, 1998).

The PMMA/ATH acrylic casting dispersion is a composite used as a substitute for many indoor household ceramics. The PMMA/ATH combines the ease of molding of PMMA with stiffness and wear resistance improvement provided by the reinforced particles of ATH. The composite materials studied in this work can be mixed with various additives to gain better visual properties, yet each one has a different failure mechanism. One relatively demanding application of this composite is as kitchen countertop. When these countertops are provided with a cutout for appliances such as a cooking stove, they are generally rectangular in shape. There are potential problems with the sharp corners of the cutout. The corners act as stress risers. Appliances that cycle through high and low temperatures, especially cooking ranges, experience thermal cycling, which induces cyclical expansion and contraction of the countertop. Depending on conditions, this thermal cycling eventually lead to cracks forming in the countertop corners that then propagate out into the countertop and cause failure. PMMA/ATH is also used to fabricate

kitchen sinks and bathroom vanities. These products also are subjected to severe temperature changes due to alternating flows of hot and cold water. Again, these temperature variations give rise to high thermal stresses, which sometimes lead to failure by cracking in the region near the drain hole. PMMA/ATH has also been popular in many other engineering applications because of its low production cost and significantly improved material properties. Recent studies of the sinks made of PMMA/ATH indicate that cracks generally occur close to the waste hole placed on the bottom of the sinks as shown in Fig. 1. The cause of these fractures seems to be the thermal stresses originating by severe temperature variations that occur when alternated flows of cold and hot water are applied.

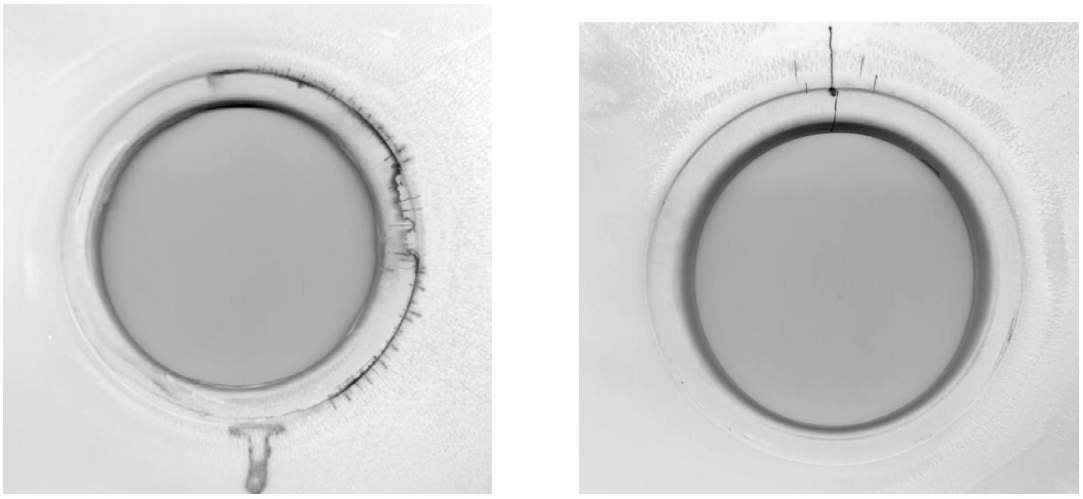

(a) (b)

Fig. 1 Cracks near the drain hole were caused by alternate cold (22^{o}C) and hot (88^{o}C) water

The mechanical behavior of particulate composites is significantly affected by the nature of the bond between the reinforcing particles and the matrix material. In most analytical

and numerical work it has been assumed that the bond is perfect and can be modeled by continuity of tractions and displacements across a discrete interface (Ju and Chen, 1994; Ju and Sun, 2001). Within the perfect interface conditions, the primary achievement is the well-known Eshelby (1957) solution of the ellipsoidal inclusion problem. Internal defects and imperfect interface however are well known to exist in composites and incorporation of such phenomena in the general theory requires the modification and relaxation of the continuity of displacements between the constituents. Clearly such an interface imperfection may significantly affect the mechanical properties and failure mechanisms as well as the strength of the particulate composites. And the influence of an interfacial zone on composite mechanical and thermal behavior has been investigated by a number of authors. There exist several investigations in literature which concentrate on the effect of imperfect interfaces in composites, such as Benveniste (1985), Achenbach and Zhu (1989, 1990), Hashin (1990, 1991).

The main aim of this work is to investigate the mechanisms of failure in PMMA/ATH using *in situ* observations during mechanical loadings at different temperatures and strain rates. The purpose of this experimental study is to lay the ground work for the following constitutive modeling stage of this project.

2. EXPERIMENTAL PROCEDURES

The tensile and compressive tests were undertaken in a servo-mechanical MTS Machine type 858 Table Top Material Characterization System (10 kN capacity) controlled by a computer and fitted with an ATS 7510 thermal chamber for the control of ambient temperature. This test system has load, stroke and strain control capacity. The accuracy of

temperature control was about 1^{o}C and was monitored by using an ATS feedback control system and a thermocouple. The test system also includes an interchangeable 685.22 side-loading hydraulic wedge grip system with grip pressure up to 3000 psi. The hydraulically actuated grip system is independently activated and can maintain an adjustable grip force on the specimen grip face without backlash. Grips are attached to the load frame via a fixed, but adjustable, commercially available alignment system. The MTS 634.25 axial extensometer (from +50% to –10%), with the gauge length of 50mm, is used to measure uniaxial strain in the specimen. The experiments were conducted as a function of strain rate and temperature for uniaxial tension and compression testing. The strain rate ranged over three decades from 1×10^{-3} to 1×10^{-5} sec^{-1}, and temperatures varied from room temperature to 90^{o}C. The details of the procedure used in this work are described in ASTM D 638-98. The specimen geometry used in these tests is shown in Fig. 2(a). Because most brittle materials are sensitive to the preexisting flaws, Duck® tape was used on the specimen at the areas where the extensometer was clipped, to protect the specimen from flaws introduced by the blade of the extensometer. Great care is taken to reduce the experimental errors which can arise from poor specimen alignment, thermal distortion of the strain extensometer arms, nonuniform heating of the test specimen, and variation in the initial loading rate. Moreover, maximum compression stress applied on the specimen was 77MPa. Euler buckling load for the specimen is 180MPa.

Nano indentation was used to measure room temperature elastic modulus of the composite. Known as depth-sensing indentation, Nano indentation employs a high resolution actuator to force an indenter into a test surface, and a high resolution sensor to continuously measure the resulting penetration. Based on the indentation load

displacement data, it can measure the material properties such as hardness and Young's modulus. Three sets of experiments were performed using Nano indenter® XP on three orthogonal polished sections for measurement of the modulus and hardness in these three directions respectively. This specimen is shown in Fig. 2(b).

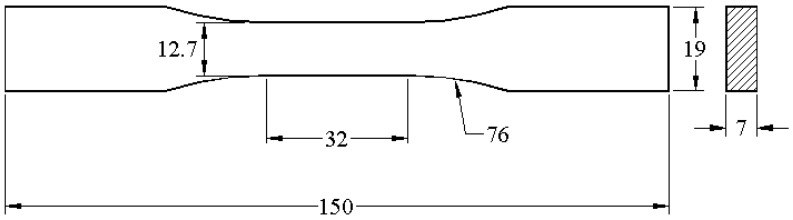

(a)

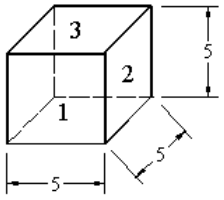

(b)

Fig. 2 Specimen geometries (mm): (a) uniaxial tests; (b) Nano indenter tests

3. RESULTS AND DISSUSSION

3.1. Failure Mechanism

The PMMA/ATH acrylic casting dispersion is known to accumulate considerable scattered microscopic damage in its service life. In particulate composite materials usually the compression and shear strength is improved. However, fillers often decrease the tensile strength. This low tensile stress and unfavorable combination of such properties as low thermal conductivity and relatively high Young's modulus render

PMMA/ATH highly susceptible to failure under a service loading condition which promotes the generation of high magnitude thermal stresses. It is well established that the fracture of particulate composites can be due to interfacial debonding between the matrix and particles, or particle cracking, or the ductile plastic failure in the matrix depending on the relative stiffness and strength of the two constituent materials and the interface strength. If the intergranular strength of the filler particles is lower than interfacial strength, usually filler particle cracking dominates failure mechanism. On the other hand, if the embedded particles are much stiffer and stronger than the matrix, matrix cracking (or cavity formation) and particle/matrix interface debonding become the major damage modes.

In order to study the effects of interfacial strength on the failure mechanism, PMMA/ATH studied in this work was prepared using lightly cross-linked poly-methyl methacrylate (PMMA) filled with alumina trihydrate (ATH) with different interfacial strength properties between PMMA and ATH. Table 1 presents the chemical and physical compositions of the materials studied. The strength of interfacial adhesion of PMMA/ATHa is much stronger among after adding adhesion promoting additives to surface of ATH; the strength of interfacial adhesion of PMMA/ATHd is much weaker after adding the debonding promoting additives to the surface of ATH.

Table 1 The chemical and physical composition of the materials tested

Material	Particles Coating	Constituents & Volume Fraction		Average Particles Size
		Matrix (PMMA)	Particles (ATH)	
PMMA/ATHa	Adhesion Promoting Additives DuPont CA-14 *	52%	48%	35 μm
PMMA/ATHd	Debonding Promoting Additives DuPont CA-11 **	52%	48%	35 μm

* US Patent 5, 708, 066, (Othemba et al., 1998).
** US Patent 5, 079, 279, (Hayashi and Kameda, 1992)

Very often, perfect adhesion is assumed between the filler and the polymer matrix as well as perfect dispersion of the individual filler particles in particulate composites. Filler particles used in PMMA/ATH composite are made up of smaller crystals as seen in Fig. 3 and Fig. 4.

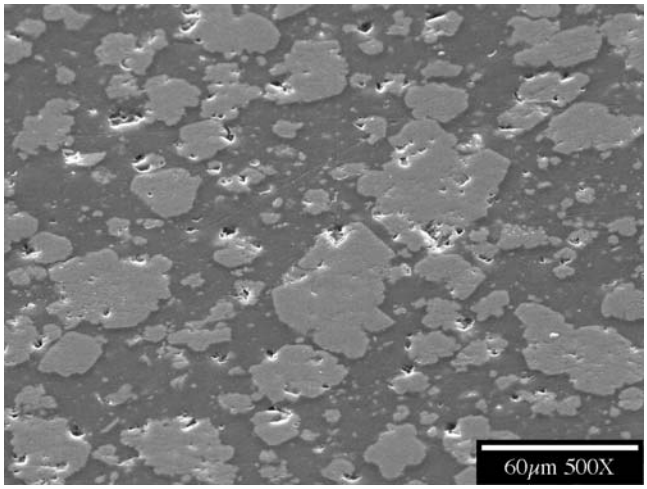

Fig. 3 SEM images of polished surface of PMMA/ATH.

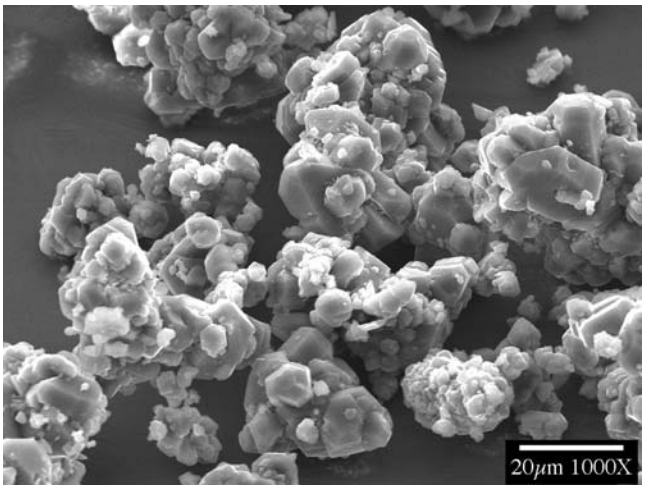

Fig. 4 SEM images of filler particles in the PMMA/ATH are agglomerates which are clusters of ATH crystals.

Figures 5-8 show the tensile fracture surfaces of the PMMA/ATHa at various temperatures. Figures 9-11 show the SEM images of the fracture surfaces of PMMA/ATHd. SEM inspection of fracture surfaces testifies that the interfacial strength has a great influence on the failure mode of particulate composites. Upon loading at a critical strain level, the agglomerates of the ATH filler particles crack at intergranular level for PMMA/ATHa. But in the case of PMMA/ATHd the agglomerates were pulled out off the PMMA matrix. Inspection of SEM images of broken surface provide the evidence that the interfacial strength of PMMA/ATHa is greater than that of the agglomerates of the ATH particles, but the interfacial strength of PMMA/ATHd is weaker than that of the agglomerates of the ATH particles. After decoupling between the filler/matrix, the PMMA matrix then deforms more than the ATH filler so that elliptical cavities or voids develop around each filler particle. Application of strain in the last region of the curve is only to stretch the PMMA and enlarge existing cavities, which is believed to consequently cause the volume growth during loading. Such phenomenon has

been studied by many researchers such as Ravichandran and Liu (1995), Kwon et al. (1997, 1998). These studies investigated the nonlinear constitutive response of a damaged particulate composite in terms of the change in volume dilation and showed that the stress-strain response is nearly linear when there is little or no volume dilatation and the non-linearity sets in once the dilatation becomes significant.

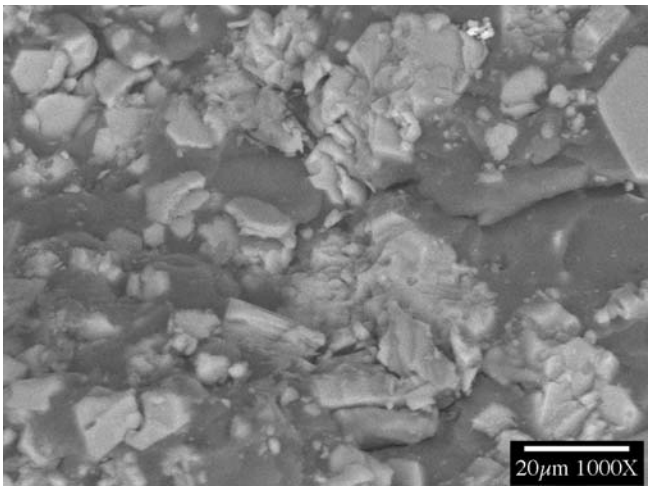

Fig. 5 The tensile fracture surfaces of PMMA/ATHa at 24 ^{0}C

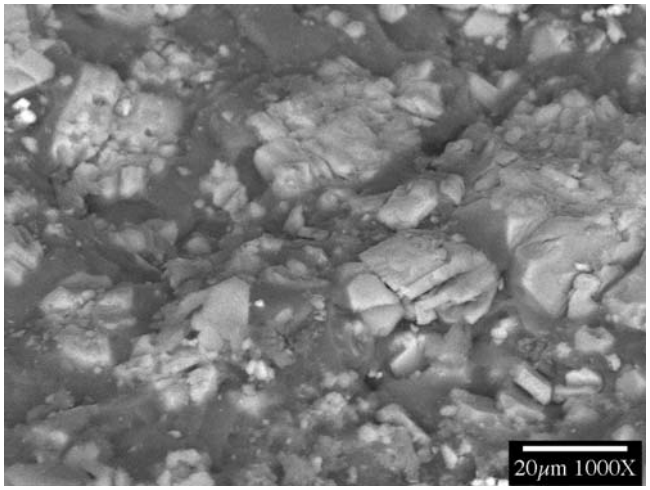

Fig. 6 The tensile fracture surfaces of PMMA/ATHa at 50 ^{0}C

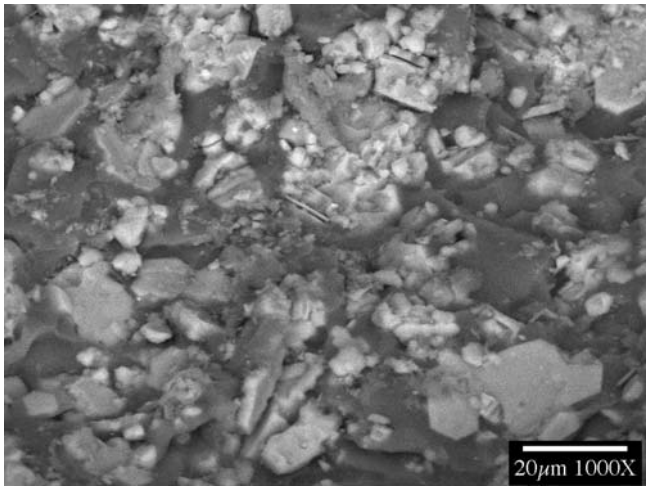

Fig. 7 The tensile fracture surfaces of PMMA/ATHa at 75 ^{0}C

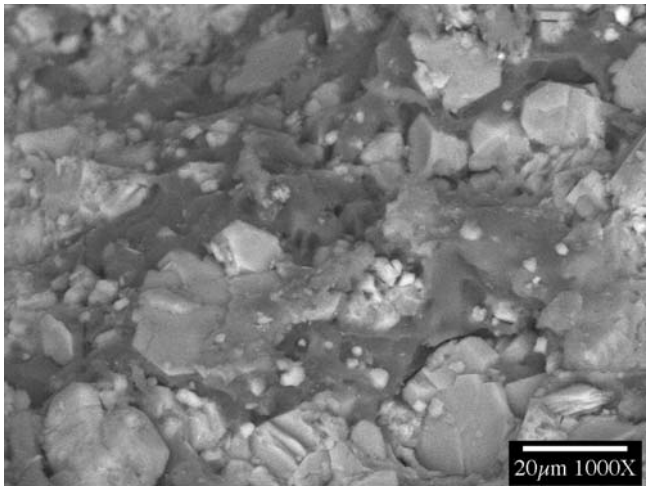

Fig. 8 The tensile fracture surfaces of PMMA/ATHa at 90 ^{0}C

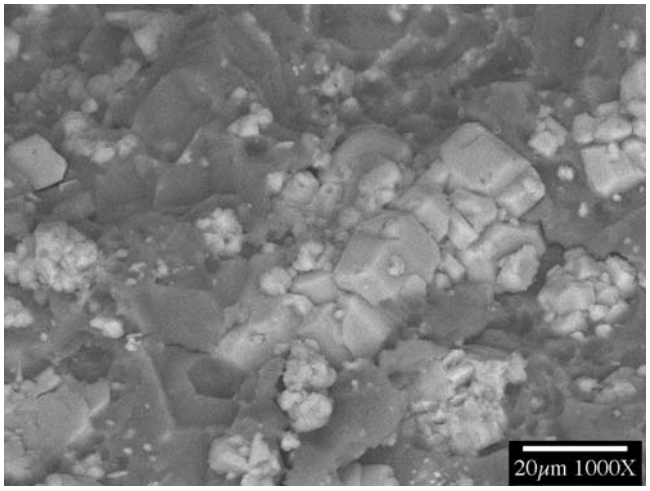

Fig. 9 The tensile fracture surfaces of PMMA/ATHd at 24 ^{0}C

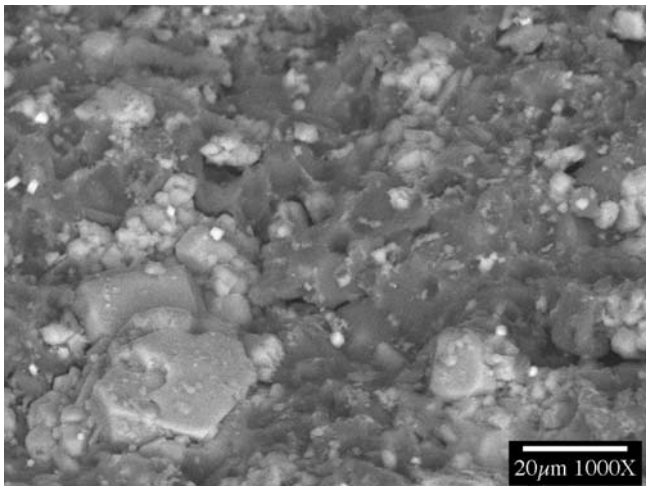

Fig. 10 The tensile fracture surfaces of PMMA/ATHd at 50 ^{0}C

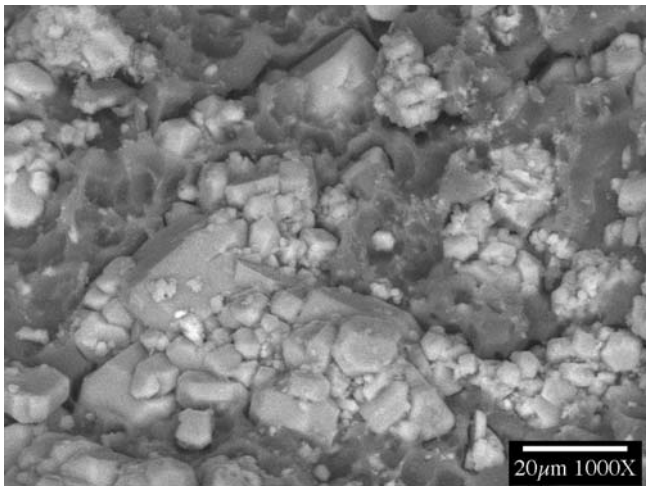

Fig. 11 The tensile fracture surfaces of PMMA/ATHd at 75 ^{0}C

The mechanism of microdamage at particulate level in PMMA/ATHa passes at least through two different stages of damage. The first being the breaking up of aggregates of ATH and the second being the fracture of the matrix. Fig. 12 illustrates this process. The mechanism of microdamage at particulate level in PMMA/ATHd also occurs at least through two different stages of damage. The first being the adhesive debonding of the

matrix from the filler and the second being properly the fracture of the matrix as shown Fig. 13 (Moshev and Evlampieva, 1997). Clearly, the debonding or particle fracture diminishes the resistance of the structural element. However, the matrix retains a capability to resist the extension for some time, although at a lower modulus. Only after the matrix part of the element has been broken, may one consider that resistance has completely vanished.

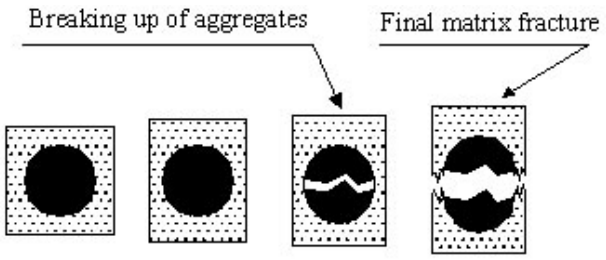

Fig. 12 Schematic of microdamage evolution in PMMA/ATHa

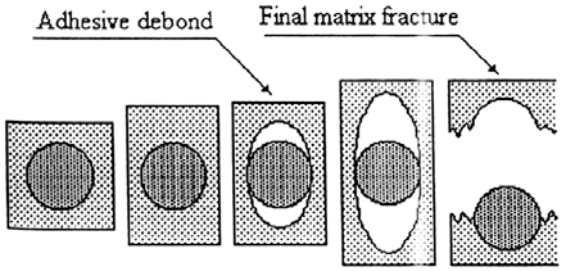

Fig. 13 Schematic of microdamage evolution in PMMA/ATHd

Typical stress-strain curves obtained from the uniaxial tension and compression tests of PMMA/ATHa at 24^{o}C are shown in Figures 14-15 for several strain rates. It is observed that yield stress in tension is much lower than that in compression. The PMMA/ATHa exhibits markedly different inelastic behavior in tension and compression, which is due to the particulate reinforcement. The microstructure of PMMA/ATHa consists of a distribution of ATH agglomerates in a PMMA matrix. In tension, the ATH filler particles

act as stress concentrators, while in compression the filler particle transmit stresses. The resulting material is brittle in tension, but in compression it is similar in behavior to PMMA matrix. The modulus in tension also has strong strain amplitude dependence in which above critical amplitude of strain the modulus shows a rapid decrease. The failure of the composite in tensile loading occurs in several stages. The stress-strain curve is initially linear elastic to a critical stress (about 25MPa) then it starts to behave nonlinearly. After the continuous nonlinear behavior, the stress-strain curve reaches the peak point and the failure of the specimen occurs suddenly before a significant plastic strain is achieved. An important effect of the strain rates on the stress-strain curve was also observed. As the applied strain rate increased, the specimen experienced a greater stress under the same applied strain level in proportion to the increased stiffness.

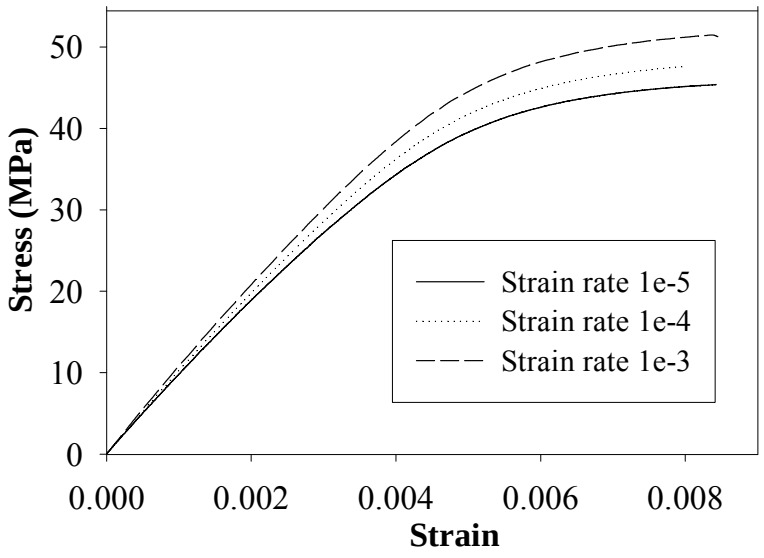

Fig. 14 Tensile stress-strain curves of PMMA/ATHa at 24 ^{0}C (to failure)

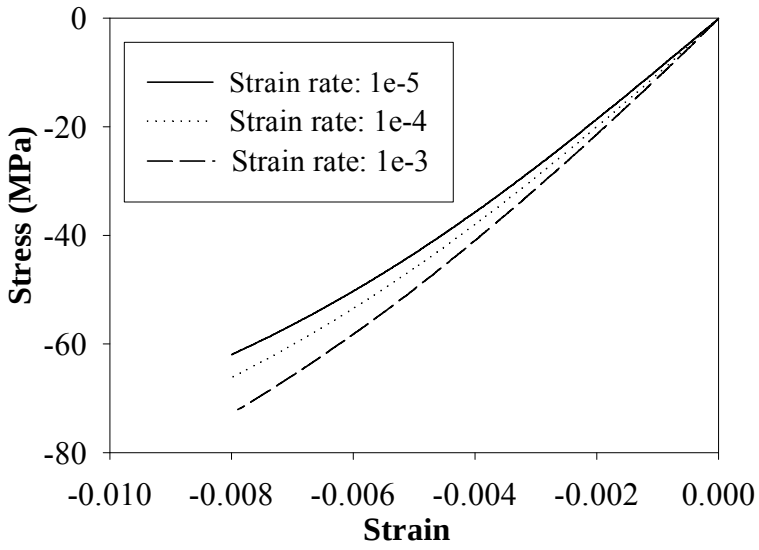

Fig. 15 Compressive stress-strain curves of PMMA/ATHa at 24 ^{0}C to strain of -0.8%

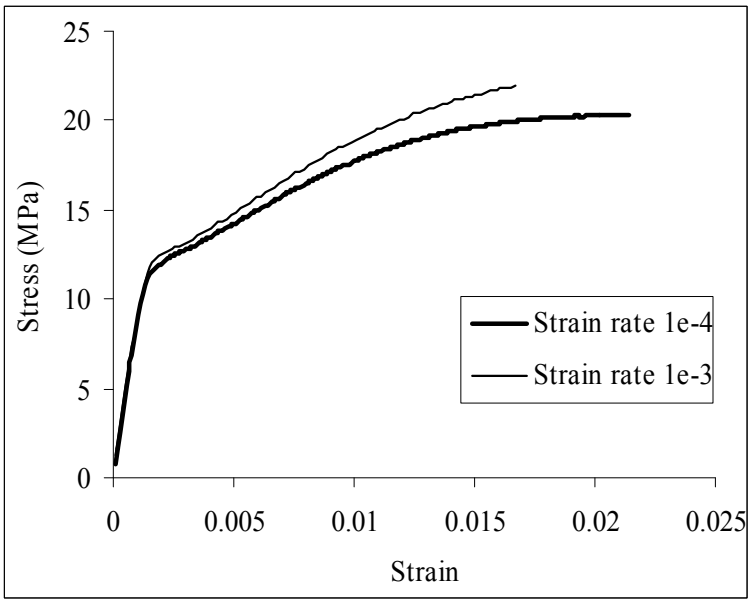

Fig. 16 Tensile stress-strain curves of PMMA/ATHd at 24 ^{0}C (to failure)

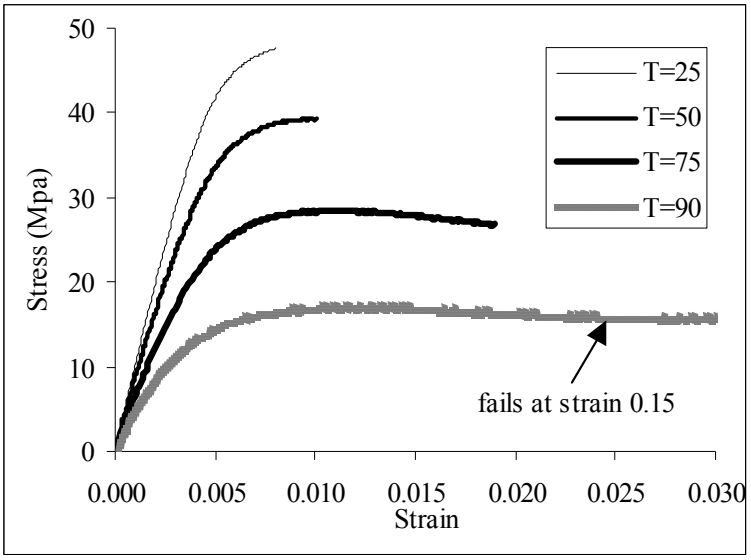

Fig. 17 Tensile stress-strain curves of composite PMMA/ATHa at different temperatures (Celsius scale)

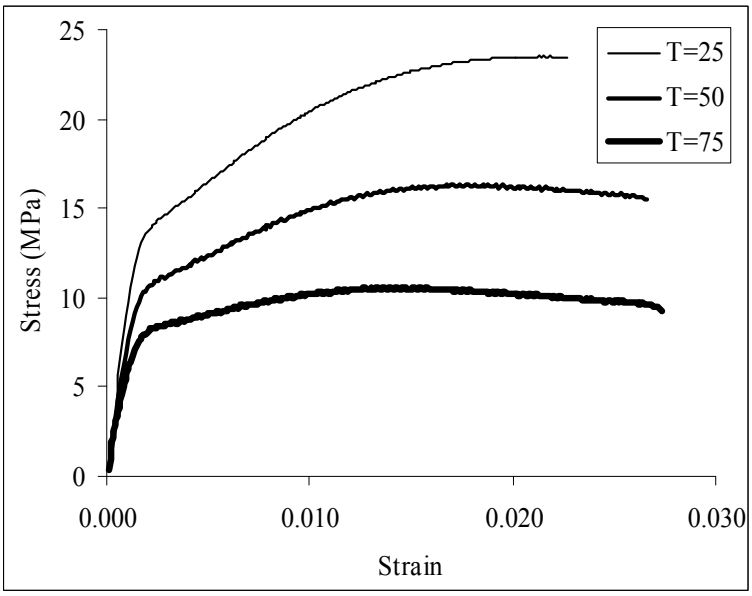

Fig. 18 Tensile stress-strain curves of composite PMMA/ATHd at different temperatures (Celsius scale)

Fig. 16 shows the stress-strain curve for PMMA/ATHd at two different strain rates. As expected, higher strain rate yields higher strength.

Fig. 17 shows stress-strain response of PMMA/ATHa at different temperatures. Even though the composite is relatively brittle at room temperature, it becomes very ductile at elevated temperatures. The glass transition temperature for the matrix is 100^{o}C.

Fig. 18 shows the stress-strain curve for PMMA/ATHd at different temperatures. This composite material behaves in a ductile manner at room temperatures and above.

3.2. Nano Indenter Tests

Using load control method, three sets of experiments were performed using Nano indenter® XP on three polished sections of a cube made of PMMA/ATHa to measure the modulus and hardness in the three orthogonal directions. Table 2 and Table 3 list the results of experiments at room temperature including the standard deviation, coefficient of variation values calculated from nine indentations for each section.

Table 2 Young's modulus at 24 ^{0}C from Nano indenter® tests

	Modulus (GPa)		
	Section 1	Section 2	Section 3
Mean	9.368	9.079	9.257
Std. Dev.	1.999	0.974	0.991
% COV	21.34	10.73	10.17

Table 3 Hardness at 24 ^{0}C from Nano indenter® tests

	Hardness (GPa)		
	Section 1	Section 2	Section 3
Mean	0.264	0.231	0.240
Std. Dev.	0.036	0.010	0.021
% COV	13.49	4.12	8.79

These results show that the mechanical properties in all directions are almost the same and the PMMA/ATH acrylic casting dispersion can be regarded as an isotropic material. The results obtained from Nano indentation are also comparable with that are obtained by uniaxial tensile tests (Fig 19).

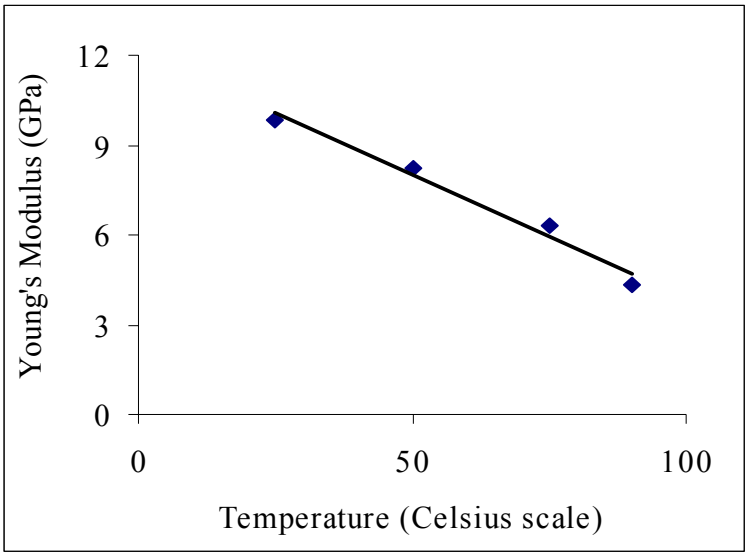

Fig. 19Young's modulus as a function of temperature

3.3 Comparison between Flexural and Tensile Tests

The ultimate strength as measured using flexural and tensile testing of PMMA/ATHa is found to be different at room temperature. This difference is attributed to the different loading types used in the corresponding tests.

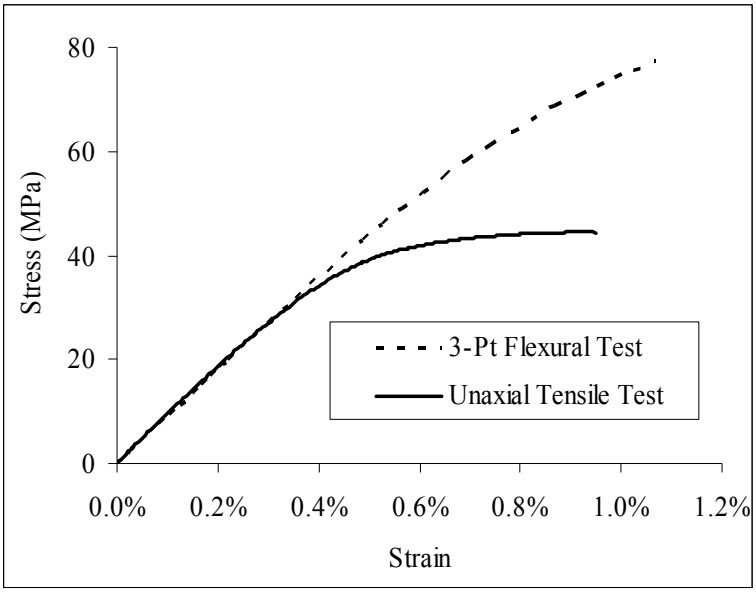

Fig. 20 Comparison of stress-strain curve of composite PMMA/ATHa between uniaxial test and 3-point bending test at room temperature

The general features of the stress-strain curves for flexural and tensile tests are shown in Fig. 20. On each of the plots an apparent stress scale is indicated. For the flexure test this stress refers to the maximum tension (or compression) stress calculated from the measured load using the relation for a uniform linear-elastic beam in bending. For the tension test the apparent stress is obtained from the measured load divided by the cross-sectional area of the test section. In both tests an initial linear elastic region is followed by nonlinear load increase to a maximum. The onset of nonlinear deflection occurred at about the same stress, 25MPa. Although the general appearance of the stress-strain curves for flexure and tension are similar, several important details differ. The peak apparent stress was surprisingly higher in bending than in tension (76MPa vs. 48MPa). These curves also differ in strains in the regions of linear load increase and nonlinear load increase. Therefore, calculation of the work done by the loading system to cause failure

(i.e., work of fracture) clearly does not give the same quantity, which is supported to be a material property independent of loading configuration.

In view of Marshall (1985), both the flexure and tension tests the onset of nonlinear deflection coincided with the formation of microporous zone (or crack) in the PMMA/ATHa. In the tension test, this zone passes completely through the central section of the specimen , and the applied load is supported entirely by the binder in this zone. A large part of the additional deformation is believed due to the deformation of the microporous zone. The response in the flexure test is similar, except that the microporous zone penetrated only to about the midplane of the beam. The formation of microporous zone in the matrix in only half of the flexure beam has important consequences. In particular, the microspores destroy the macroscopic uniformity of the beam and render calculation of stress based on a uniform linear elastic beam invalid. Consequently, flexural tests as also suggested by Marshall (1985) should not be used for the determination of ultimate strength, although it can be used for measurement of stress and formation of a microporous zone.

4. CONCLUSIONS

The influence of the interfacial bond strength between particles and the matrix on the failure mechanism of acrylic casting dispersion has been investigated using *in situ* observations during uniaxial loadings conditions. It is suggested that macroscopic fracture is initiated in the clusters of the reinforcing particles when the interfacial bond between particles and matrix is very strong. For weak interfacial bond strength, the macroscopic fracture is initiated by debonding of clusters of the reinforcing particles.

Flexural tests can be used for measurement of the stress before a microporous zone (or crack) in the matrix is formed. However, once the first crack forms the uniformity of the beam is destroyed and the stresses in the beam are no longer related solely to the applied load and the specimen dimension. The relation between the peak load and the failure stress is obscure. Consequently, flexural tests should not be used as a substitute for measurement of ultimate tensile strength.

5. ACKNOWLEDGEMENTS

Support by Dupont Surfaces is greatly appreciated. The fourth author was a visiting researcher in Department of Civil, Structural and Environmental Engineering, University at Buffalo, State University of New York.

REFERENCES

Achenbach, J.D. and Zhu, H. (1989) "Effect of Interfacial Zone on Mechanical Behavior and Failure of Fiber-Reinforced Composites", *J. Mech. Phys. Solids,* Vol. 37, No.3 pp. 381-393.

Achenbach, J.D. and Zhu, H. (1990). "Effect of Interphases on Micro and Macromechanical Behavior of Hexagonal-Array Fiber Composites", *Transaction of the ASME, Journal of Applied Mechanics,* Vol. 57, pp. 956-963.

American Society for Testing and Materials, Standard Test for Tensile Properties of Plastics, *Annual Book of ASTM*, Vol. 08.01, ASTM D 638-98 (1999).

Benveniste, Y. (1985). “The Effective Mechanical Behavior of Composite Materials with Imperfect Contact between the Constituents”, Mechanics of Materials, Vol. 4, pp. 197-208.

Chawla, K. K. (1998). *Composite Materials: Science and Engineering*, 2nd edition, Spring-Verlag, New York, 1998.

Eshelby, J.D. (1957). *Proceedings of the Royal Society of London, Series A*, Mathematical Science, Vol. 241, Issue 1226, pp376-396.

Hashin, Z. (1990) “Thermoelastic Properties and Conductivity of Carbon/Carbon Fiber Composites”, *Mechanics of Materials*, Vol.8, pp293-308.

Hashin, Z. (1991) “The Spherical Inclusion with Imperfect Interface”, *Transaction of the ASME, Journal of Applied Mechanics,* Vol. 58, pp. 444-449.

Hayashi, T. and Kameda, K. (1992). Reaction Curable Resin Composition and Artificial Marble, US Patent 5,079,279

Ju J. W. and Chen (1994), "Micromechanics and Effective Moduli of Elastic Composites Containing Randomly Dispersed Ellipsoidal Inhomogeneities", *Acta Mechanica* 103, pp. 103-121.

Ju J. W. and Sun, L. Z. (2001). "Effective Elastoplastic Behavior of Metal Matrix Composites Containing Randomly Located Aligned Spheroidal Inhomogeneities. Part I: Micromechanics-Based Formulation", *International. Journal of Solids and Structures*, Vol. 38, pp.183-201

Kwon, Y. W., Lee, J. H. and Liu, C. T. (1997). "Modeling and Simulation of Crack Initiation and Growth in Particulate Composites", *Journal of Pressure Vessel Technology*, Vol. 119, pp319-324.

Kwon, Y. W., Lee, J. H. and Liu, C. T. (1998). "Study of Damage and Crack in Particulate Composites", *Composites Part B: Engineering*, Vol. 29, No. 4, pp. 443-450.

Marshall, D. B. and Evans, A.G. (1985). "Failure Mechanism in Ceramic-Fiber/Ceramic-Matrix Composites", *Journal of the American Ceramic Society*, Vol. 68, No. 5, pp.225-31.

Moshev, V. V. and Evlampieva, S. E. (1997). "Discrete Models of Failure for Particulate Polymer Composites", *Polymer Engineering and science*, Vol. 37, No.8, pp.1248-1358.

Otremba E. D., Friscia, R. M., McBride, E. F. (1998). Reaction Curable Composition and Solid Surface Material, US Patent 5,708,066

Ravichandran, G. and Liu, C. T. (1995). "Modeling Constitutive Behavior of Particulate Composites Undergoing Damage", *International Journal of Solids and Structures*, Vol. 32, No. 6/7, pp.979-990.